

# Size and asymmetry of the reaction entrance channel: influence on the probability of neck production

P.M.Milazzo<sup>a</sup>, G.Vannini<sup>b</sup>, C.Agodi<sup>c</sup>, R.Alba<sup>c</sup>, G.Bellia<sup>c</sup>,  
 N.Colonna<sup>d</sup>, R.Coniglione<sup>c</sup>, A.Del Zoppo<sup>c</sup>, P.Finocchiaro<sup>c</sup>,  
 F.Gramegna<sup>e</sup>, I.Iori<sup>f</sup>, C.Maiolino<sup>c</sup>, G.V.Margagliotti<sup>a</sup>,  
 P.F.Mastinu<sup>e</sup>, E.Migneco<sup>c</sup>, A.Moroni<sup>f</sup>, P.Piattelli<sup>c</sup>, R.Rui<sup>a</sup>,  
 D.Santonocito<sup>c</sup>, P.Sapienza<sup>c</sup>.

<sup>a</sup>*Dipartimento di Fisica and INFN, Trieste, Italy*

<sup>b</sup>*Dipartimento di Fisica and INFN, Bologna, Italy*

<sup>c</sup>*INFN, Laboratori Nazionali del Sud, Catania, Italy*

<sup>d</sup>*INFN, Bari, Italy*

<sup>e</sup>*INFN, Laboratori Nazionali di Legnaro, Italy*

<sup>f</sup>*Dipartimento di Fisica and INFN, Milano, Italy*

---

## Abstract

The results of experiments performed to investigate the Ni+Al, Ni+Ni, Ni+Ag reactions at 30 MeV/nucleon are presented. From the study of dissipative mid-peripheral collisions, it has been possible to detect events in which Intermediate Mass Fragments (IMF) production takes place. The decay of a quasi-projectile has been identified; its excitation energy leads to a multifragmentation totally described in terms of a statistical disassembly of a thermalized system ( $T \simeq 4$  MeV,  $E^* \simeq 4$  MeV/nucleon). Moreover, for the systems Ni+Ni, Ni+Ag, in the same nuclear reaction, a source with velocity intermediate between that of the quasi-projectile and that of the quasi-target, emitting IMF, is observed. The fragments produced by this source are more neutron rich than the average matter of the overall system, and have a charge distribution different, with respect to those statistically emitted from the quasi-projectile. The above features can be considered as a signature of the dynamical origin of the midvelocity emission. The results of this analysis show that IMF can be produced via different mechanisms simultaneously present within the same collision. Moreover, once fixed the characteristics of the quasi-projectile in the three considered reactions (in size, excitation energy and temperature), one observes that the probability of a partner IMF production via dynamical mechanism has a threshold (not present in the Ni+Al case) and increases with the size of the target nucleus.

## 1 INTRODUCTION

The production of intermediate mass fragments (IMF,  $Z \geq 3$ ) is one of the main features of the nuclear reactions in the Fermi energy regime (i.e. at bombarding energies of 30-50 MeV/nucleon), and can arise from various mechanisms [1].

Compound systems, formed in central collisions, break into several IMFs. This behaviour has been described in terms of a statistical approach in which low density nuclear matter is supposed to have a liquid-gas phase transition [2]. In fact the experimental observables, charge distribution and partition, and the shape of the caloric curve (temperature versus excitation energy) [3] are in good agreement with the predictions of such statistical multifragmentation models [4].

At these energies in peripheral and midperipheral collisions, it has been observed that the quasi-projectile (QP) and the quasi-target (QT), can de-excite following a statistical pattern and giving rise to the production of IMF.

On the other hand, many experiments have shown that at mid-rapidity dynamical mechanisms lead to the production of IMF; this effect is due to the rupture of a neck-like structure joining QP and QT [5,6]. Various transport calculations predict that dynamical fluctuations dominate the neck instability allowing the production of IMF [7]; moreover the experimental results (in particular concerning the charge distribution and the isotopic composition of fragments) can not be described in terms of statistical approaches.

It has been shown that in midperipheral collisions it is possible to observe inside the same event the competition between statistical and dynamical mechanisms leading to the production of IMF [6].

To better investigate this phenomenon we experimentally studied the Ni+Al, Ni+Ni, Ni+Ag midperipheral collisions at 30 MeV/nucleon. The results of this investigation are presented and discussed in this paper.

At first, within the same set of mid-peripheral events, we separate the IMFs coming from the statistical disassembly of the QP from those coming from a dynamically driven neck rupture. Then, we study the balance between these two mechanism of IMF production for the three different interacting systems. The comparison between the IMF produced via statistical and dynamical processes show significant differences concerning the charge distributions and the isotopic composition of the fragments. The analysis of the different systems will demonstrate that the neck formation probability is strongly influenced by the size of the target.

In Sect.2 a description of the experimental conditions is given; the mid-peripheral collisions features are discussed in Sect.3; Sect.4 is devoted to the analysis of the QP emitting source formed in the three different reactions studied. The production of IMF at midvelocity is discussed in Sect.5, then the conclusions are drawn in Sect.6.

## 2 EXPERIMENTAL SET-UP AND DATA ANALYSIS PRESCRIPTIONS

The experiment was performed at the INFN Laboratori Nazionali del Sud, where the superconducting cyclotron delivered a beam of  $^{58}\text{Ni}$  at 30 MeV/nucleon, using the MEDEA [8] and MULTICS [9] experimental apparatus as detectors. The angular range  $3^\circ < \theta_{lab} < 28^\circ$  was covered by the MULTICS array [9], which consists of 55 telescopes, each made of an Ionization Chamber (IC), a Silicon position-sensitive detector (Si) and a CsI crystal. The typical values of the energy resolutions are 2%, 1% and 5% for IC, Si and CsI, respectively. The identification threshold in the MULTICS array was about 1.5 MeV/nucleon for charge identification. Good mass resolution for light isotopes (up to Carbon) was obtained. Energy thresholds for mass identification of 8.5, 10.5, 14 MeV/nucleon were achieved for  $^4\text{He}$ ,  $^6\text{Li}$  and  $^{12}\text{C}$  nuclei respectively. The  $4\pi$  detector MEDEA is made of 180 Barium Fluoride detectors placed at 22 cm from the target and it can identify light charged particles ( $Z=1,2$ ) ( $E \leq 300$  MeV) and  $\gamma$ -rays up to  $E_\gamma=200$  MeV in the polar angles from  $30^\circ$  to  $170^\circ$  and in the whole azimuthal angle [8].

In these experiments light charged particles and fragments were detected on an event by event basis, thus allowing the description of the reaction dynamics.

In heavy ions reactions at intermediate energies different decaying systems are formed, depending on the impact parameter, and become the source of fragments which differ in size, shape, excitation energy, and in the way they are formed. Therefore one must identify the decaying systems and ensure that all the fragments are correctly assigned to one of these systems. Thus, since the aim of this paper is to present data on IMF production in the following we will restrict our analysis only on many-fragments events [6]. Since however many fragments can be produced both in central and midperipheral collisions, it is mandatory to distinguish collisions occurred at different impact parameters, in order to have a comprehension of the mechanisms responsible for IMF production and emission

The impact parameter data selection is based on the heaviest fragment velocity. We can select peripheral and midperipheral events when the heaviest fragment (produced by the disassembly of a QP emitting source) in the laboratory frame travels at velocities higher than 80% of that of the projectile ( $v_P=7.6$  cm/ns); on the contrary, in central collisions the heaviest fragment travels at velocities close to that of the centre of mass. Only “complete” events are analyzed, i.e. when at least 3 IMF are produced (with the heaviest fragment having  $Z \geq 9$ ) and more than 80% of the total linear momentum is detected. Accordingly, since the energy thresholds prevent from detecting the QT reaction products, we find that the total detected charge ( $Z_{Tot}$ ) does not differ from that of the projectile for more than 30% ( $20 \leq Z_{Tot} \leq 36$ ).

## 3 DYNAMICAL AND STATISTICAL IMF PRODUCTION IN MID-PERIPHERAL COLLISIONS

The results presented hereafter will refer only to mid-peripheral collision events, with at least three detected IMF, observing the IMFs emitted from the QP and from the mid-velocity neck (neck-IMF in the following), and studying the different and competitive IMF production mechanisms.

In Fig.1 the yields of carbon and oxygen fragments (for the three considered reactions) are plotted as a function of the component of the velocity parallel to the beam axis. The centre of mass velocities for the three systems are 5.18 (Al), 3.80 (Ni) and 2.65 (Ag) cm/ns.

The IMF possibly coming from the QT and part of those having mid-velocity were not detected. The problem affects the study of mid-velocity IMF mainly for the Ni+Ag reaction.

Beginning with the upper panels of Fig.1 (Ni+Al), at the centre of mass velocity there is a minimum in the production of  $Z=6-8$  fragments; this fact suggests a negligible formation of a neck-like structure for this light system. On the contrary, in Ni+Ni we notice that at mid-velocity a large contribution of IMF is present [6]. At last, the lower panels (Ni+Ag) show evidence of a larger contribution of mid-velocity IMF (even if there is a clear efficiency cut).

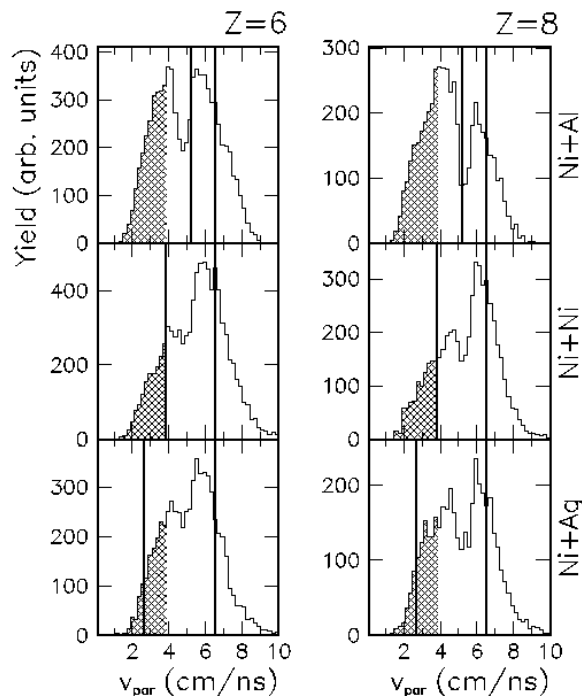


Fig. 1. Experimental  $v_{par}$  distributions for  $Z=6$  (left panels) and  $Z=8$  (right panels), for the three studied reactions; vertical lines refer to the center of mass and QP velocities. Experimental efficiency cut occurs in the shadowed area.

Thus, for mid-peripheral collisions, while the disassembly of a QP (and a QT) is present in all the three considered systems, the production of IMF at mid-velocity depends on the size of the target nucleus.

#### 4 THE IMF EMITTED FROM THE QP DECAY

To compare the reaction mechanisms for midperipheral collisions for the three different interacting systems we have to select a set of “complete” events (as described in Sec.2) for which the QPs have very similar characteristics; then, we will study the process leading to its disassembly. We will further restrict the analysis to fragments emitted with  $v_{par} > 6.5$

cm/ns (QP-IMFs in the following), forcing the selection of the QP decay products forward emitted (see for instance Fig.1), with negligible contamination due to QT and midvelocity source emission.

In order to evaluate the degree of equilibration reached by the QP before its disassembly, we measured the angular and energy distribution of the QP emitted isotopes, in their reference frame.

#### 4.1 THE QP-IMFs ANGULAR AND ENERGY DISTRIBUTIONS

The investigation of the angular distributions is also aimed at verifying if the QP fragments are produced by a nearly isotropic emitting source as expected for a statistical decay. The angular distributions of QP fragments for the three reactions are presented in Fig.2; the flat shape is in agreement with the hypothesis of an isotropic emission, a necessary condition to establish a possible equilibration of the studied system.

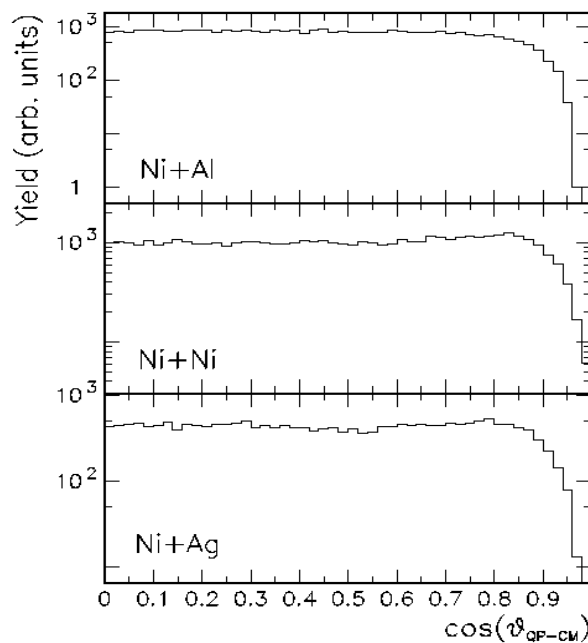


Fig. 2. Angular distributions for IMF forward emitted by the QP, for the three studied reactions. Energy distributions can be strongly influenced by the fact that Coulomb and collective energies are mass dependent; energy spectra of different isotopes may display different slopes [10]. On the contrary, the thermal energy contribution must be the same for all masses; by fitting the energy distributions with a Maxwellian function (for a surface emission)

$$Y(E) = \frac{(E - E_0)}{T_{slope}^2} \cdot e^{-\frac{(E-E_0)}{T_{slope}}} \quad (1)$$

we find comparable values of  $T_{slope}$  for all the detected isotopes ( $3 \leq A \leq 14$ ).  $T_{slope}$  is the parameter related to the apparent temperature, and  $E_0$  is a parameter related to the Coulomb

repulsion. The results are reported in Table I.

The behaviour of angular and energy distributions indicates that the condition of equilibration of the fragmenting QP systems is satisfied.

From the comparison of the QP behaviour in the three different reactions, it is possible to notice the similarity of the obtained apparent temperature slopes, independent from the considered isotope. As an example in Fig.3 the energy distribution of  ${}^6\text{Li}$  and  ${}^{10}\text{B}$  isotopes are compared; the results of the maxwellian fit are superimposed.

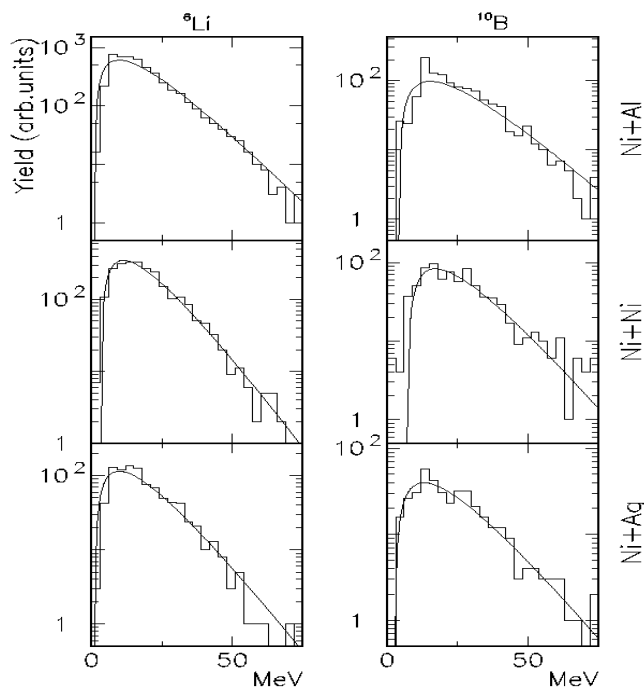


Fig. 3. Energy distributions for the  ${}^6\text{Li}$  and  ${}^{10}\text{B}$  isotopes; maxwellian fits are superimposed

#### 4.2 THE QP-IMFs CHARGE DISTRIBUTION

The following point is related to the study of the QP-IMFs charge distributions, presented in Fig.4. We have to stress that, with the adopted data selection, the distributions are quite similar; the QP mean elemental charge multiplicities of the fragments, produced in the Ni+Al and Ni+Ni cases, are overlapping, and the difference presented by the Ni+Ag case at large values of  $Z$ , is probably due to a smaller excitation energy of this QP or to a pick-up of few nucleons from the target.

#### 4.3 THE QP-IMFs ISOTOPIC COMPOSITION

Isotopic effects in nuclear reactions have recently received attention because of their relation with the symmetry energy in the nuclear equation of state [11].

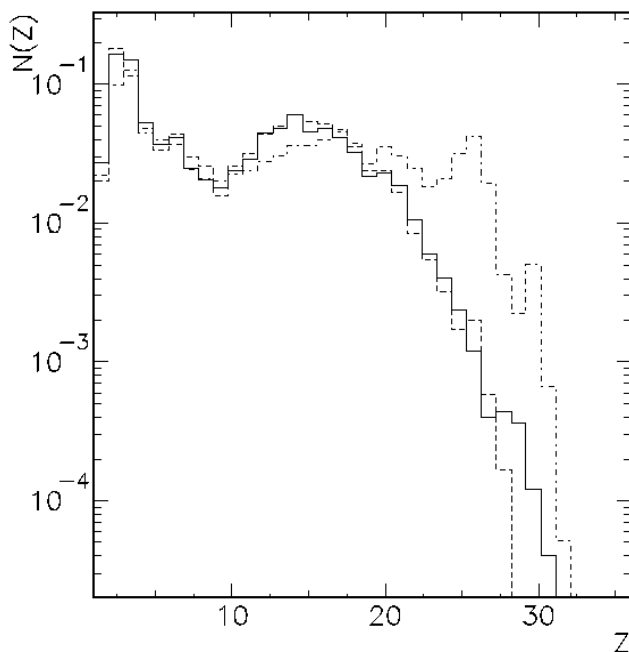


Fig. 4. Mean elemental event multiplicity  $N(Z)$  for QP charged products (full line Ni+Al, dashed line Ni+Ni, dot-dashed line Ni+Ag)

Even though the QP-IMF charge distributions present a similar shape in the three considered cases, the isotopic composition of fragments could be affected by the different  $N/Z$  ratio of the three different targets. In Table II are reported the measured isotopic composition of the QP-IMFs, expressed in percentage terms of the yields ratio  $Y(Z, A)/Y(Z)$ , for fixed  $Z$  values. No significant fluctuations can be appreciated among the three analysed reactions. It is important to stress that many experimental evidences have shown that the neck IMFs, reaction partner of the studied QPs, are neutron rich [5,6,12]. However, the QP characteristics result unchanged, with respect to those of the starting Ni projectile nucleus. To this point in Table III are presented the average values of the  $N/Z$  ratios at different  $Z$ , and they are close to the value (1.07) of the projectile Ni nucleus, and very similar to those of the stable nuclei.

#### 4.4 THE QP EXCITATION ENERGY AND TEMPERATURE

Since energy and angular distributions satisfy some necessary conditions that support the hypothesis that the QP has been subject to an equilibration process, we can investigate some of its thermodynamic characteristics (temperature and excitation energy).

For this experiment it is not possible to perform an evaluation of the excitation energy through calorimetry [13], because this technique requires a careful event by event assignment of each fragment to its emitting source [14], and here it is not possible due to the overlap of distributions between midvelocity and QP velocity. The excitation energies were therefore estimated by comparing the data with the SMM predictions [4] which best describe the experimental findings of the QP fragment emission. In Ref. [15] it is shown that quantum-molecular dynamics calculations suggest that the QP size doesn't differ significantly from

that of the projectile. The calculations were then performed for a Ni nucleus at one third of the normal density. The events generated by SMM for different input excitation energies were filtered with the experimental constraints. Experimental charge distributions were better reproduced by choosing an excitation energy of 4.0, 4.0 and 3.5 MeV/nucleon for the decaying QP in the Ni+Al, Ni+Ni and Ni+Ag, respectively (see for instance Fig.8 of Ref.[12]).

The temperature was evaluated by means of the double ratios of isotope yields [16]. The double ratio  $R$  of the yields  $Y$  of four isotopes in their ground states, prior to secondary decay is given by:

$$R = \frac{Y(A_1, Z_1)/Y(A_1 + 1, Z_1)}{Y(A_2, Z_2)/Y(A_2 + 1, Z_2)} = \frac{e^{B/T}}{a} \quad (2)$$

where  $a$  is a constant related to spin and mass values and

$$B = BE(Z_1, A_1) - BE(Z_1, A_1 + 1) - BE(Z_2, A_2) + BE(Z_2, A_2 + 1),$$

and  $BE(Z, A)$  is the binding energy of a nucleus with charge  $Z$  and mass  $A$ .

In principle,  $R$  gives directly the temperature  $T$ . However, primary fragments can be excited so that secondary decays from higher lying states of the same and heavier nuclei can lead to non-negligible distortions of the measured ratios  $R$ . In Refs.[17,18] an empirical procedure was proposed, to strongly reduce such distortions; it was shown [18,19] that for temperatures near 4 MeV these empirical correction factors do not depend either on the size or on the N/Z ratio of the decaying systems.

Moreover to apply the double ratios method [16] one has to be sure that the nuclei originate from the same emitting source and therefore, when the contributions of different sources are present, particular care must be taken in selecting the isotopes.

The break-up temperatures  $T$  of the QP decaying system were extracted averaging the values obtained from different double ratios of isotope yields, corrected as suggested in Ref.[17]. The experimental temperatures and excitation energies of the present measurements, are reported in Table IV.

#### 4.5 THE QP CHARACTERISTICS SUMMARY

In summary the adopted data selection allowed us to select the mid-peripheral collisions for which, in the exit channel of the reaction, the QP decaying systems have the same characteristics, in the three considered reactions.

In particular, the QP disassembly is well described within a statistical framework, and its properties are: a) a size close to that of the incident Ni nucleus, b) an excitation energy around 4 MeV/nucleon, c) a temperature around 4 MeV. Properties b) and c) place the system well inside the plateau of the caloric curve, where statistical multifragmentation is the main decay pattern.



## 5 THE MIDVELOCITY IMF PRODUCTION

From what shown in the previous chapter it is clear that we are working with a particular channel in which (changing the target) we have the same excitation energy for the QP nuclei. Therefore, it is interesting to investigate what happens to the midvelocity IMF production, partner in the reaction, in the three different cases. In fact, once fixed the energy dissipation process, the IMF neck production can be directly related to the different size and asymmetry of the entrance channel.

As shown in Fig.1 a large amount of IMFs are emitted at midvelocity in midperipheral Ni+Ni and Ni+Ag reactions; contribution from such emission is not sizeably present in the lighter analysed system Ni+Al. While for all the three reactions the fragmentation of the QP is very well explained in terms of statistical break-up, the presence, inside the same event, of IMF at intermediate velocity, can not be explained in terms of a pure statistical theory; different studies [5] have shown that the origin of midvelocity IMF can be considered of dynamical nature. In particular, by comparing the characteristics of the statistically emitted QP-IMFs and those of the neck IMFs, it is possible to observe how their charge distribution and isotopic composition are significantly different [6,12]; these evidences fortify the idea that two competitive reaction processes can take place simultaneously.

The characteristics of neck IMFs have been evaluated by means of fit procedures, that rely on the fact that the QP properties are well established; the characteristics of the neck IMFs are then extracted studying the deviations from statistical distributions, as described in the following. The main assumption is that fragments emitted with velocities higher than that of the QP ( $v_{QP} > 6.5$  cm/ns) origin only from the QP decay (forward emission from the QP, with negligible contribution coming from other source disassemblies).

We fitted the QP-IMFs velocity distributions taking into account only the forward emission region, by means of a gaussian function with its maximum fixed at the QP velocity. This procedure was repeated for each fragment charge in the range  $Z=3-14$  (see for instance at Fig.9 of Ref.[12]). From the results it was then possible to extract the yield  $Y_{QP}(Z)$  for each fragment emitted by the QP.

Due to the experimental energy threshold the velocity spectra are affected by detection inefficiencies. Then, we restricted our analysis to velocities higher than 3.8 cm/ns, where the distributions are not influenced by experimental cuts. This value has been chosen because the IMF emitted from the QT decay can not have velocities (in the laboratory frame) that exceed 3.5 cm/ns (this was checked by using the predictions of the Classical Molecular Dynamics model [20]). The yield of the neck IMFs ( $Y_{Neck}$  contribution) has been extracted by means of a two emitting sources fitting procedure: one source is related to the QP, and its parameters were completely determined in Sec.4, the other is centered at the centre of mass velocity and takes into account the midvelocity fragments. In the fitting procedure we used two gaussian distributions to reproduce the experimental data; there is not a physical reason to justify this choice for the dynamical component, however the results are not affected by this particular constraint. In fact, no differences were found between the present results and those already published [6,12] obtained for the Ni+Ni mid-peripheral collisions, where a direct quantitative analysis was possible.

The results for the Ni+Ag reaction are presented in Fig.5.

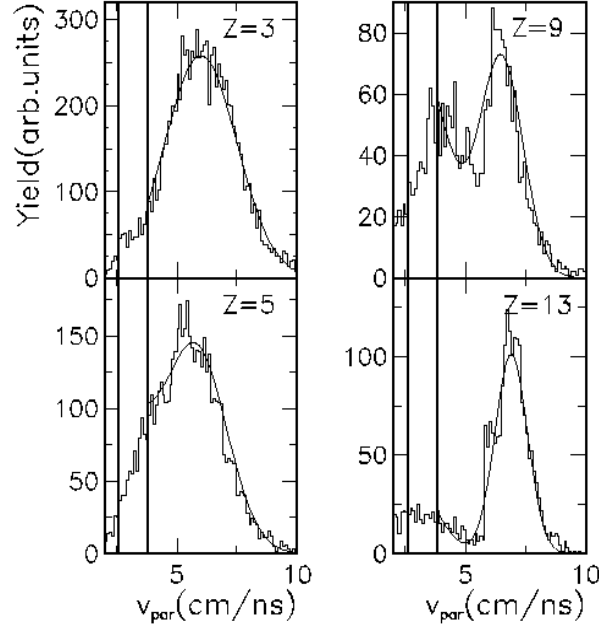


Fig. 5. Experimental Ni+Ag  $v_{par}$  distributions ( $Z=3, 5, 9, 13$ ) and superimposed fit; the lines refer to the centre of mass (2.65 cm/ns) and efficiency threshold (3.8 cm/ns)

The comparison between the total and QP-IMFs  $v_{par}$  distributions allows us to evaluate the yield ( $Y_{Neck}$ ) at midvelocity.

The IMF charge distributions (from QP and midvelocity) are very different: the IMF coming from a neck rupture mainly have charges between that of carbon and of oxygen. In order to enhance this aspect, in Fig.6a the ratio between the relative yields ( $Y_{Neck}/Y_{QP}$ ) is presented (for the Ni+Ni and Ni+Ag cases) as a function of the atomic number  $Z$ . We observe a bell-like shape, with very similar behaviour in both reactions. The fact that the maximum of this ratio is located at  $Z=9$  is due to the strong decrease of the QP charge distribution in this region (see Fig.4). It is worthwhile to notice the higher amount of neck IMFs produced in the Ni+Ag reaction. In Fig.6a the relative yield ( $Y_{Neck}/Y_{QP}$ ) for the Ni+Ni reaction is multiplied by a factor 1.862 (which is the ratio between the Ag and Ni mass (108/58)); we observe that, except for the two lighter and less probable neck IMFs, the double ratio between the relative yields is almost constant (Fig.6b) around the value  $108/58=1.862$ . This fact suggests that the size of the target nucleus plays a direct role in the amount of neck IMFs production.

In many references [5,6,12] it has been shown that the IMFs coming from a neck like structure differ from those produced in a QP decay for what concern the isotopic composition. In Fig.7 the relative yields of different isotopes are presented; it is clear that the neck IMFs are heavier in mass (for fixed  $Z$  values) than those emitted by the QP.

The energy threshold to extract the mass value of the detected fragments is higher than that allowing for charge identification; this experimental inefficiency does not permit a quantitative investigation of the isotopic composition of neck IMFs in the Ni+Ag reaction (no information is available on the mass of the fragments with velocity lower than  $\approx 5$  cm/ns). However, since the QP-IMFs forward emitted distributions are not affected by experimental

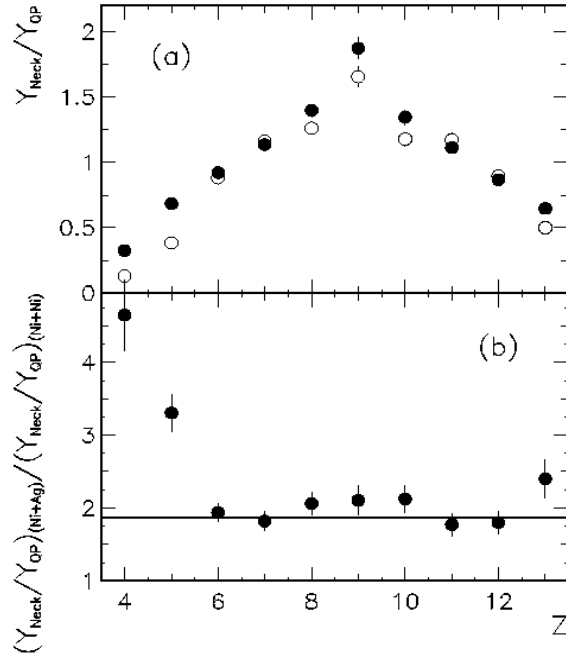


Fig. 6. (a) Upper panel: ratio of the measured yield for neck fragmentation and QP emission (open points Ni+Ni, multiplied by a factor 1.862; full points Ni+Ag); (b) lower panel: double ratio between relative yields

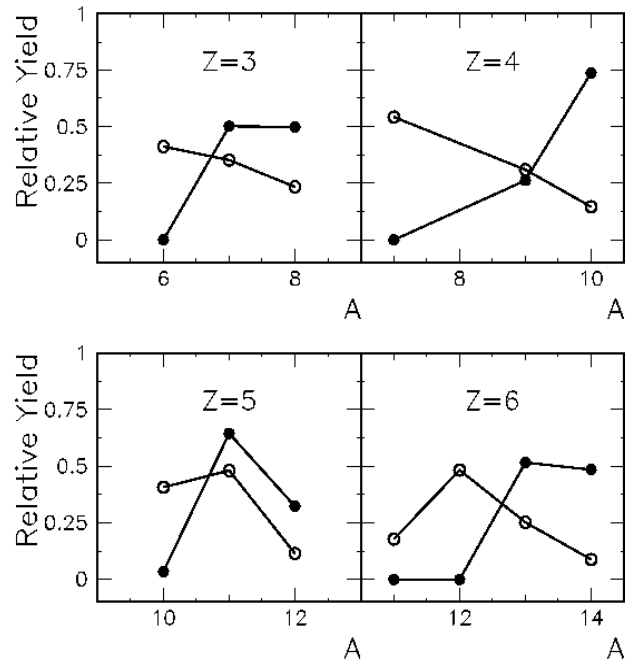


Fig. 7. Relative yields of different isotopes for fragments with charges from Z=3 to Z=6, for the Ni+Ni reaction. Open circles are related to the QP-IMFs, full circles represent the neck IMFs

cuts, we can give a qualitative evaluation of the isotopic composition of neck IMFs, looking at the very poor available data in the QP backward side (searching information by means of the comparison QP forward-backward emission). In Table V the average values of the N/Z ratio for different Z numbers are presented. The energy threshold increases with the mass of the detected nucleus. The higher identification thresholds for the heavier isotopes weakly affect the calculation of the average values of the N/Z ratio, for the Ni+Ag case. Then for this system, to be conservative, we can give only a lower limit for this ratio.

Then, not only the charge distribution, but also the isotopic composition of the neck IMFs is very similar in the two analysed systems.

In summary the IMFs emitted in dynamical processes such as the neck formation have a charge distribution and neutron contents which are very different from those emitted in statistical processes. In particular the isospin composition of the dynamically emitted IMFs is very different even from that of the total system.

## 6 CONCLUSIONS

The experimental investigation of the reactions Ni+Al, Ni, Ag 30 MeV/nucleon were performed at the Superconducting Cyclotron of the INFN Laboratori Nazionali del Sud, Catania.

In the study of the dissipative midperipheral collisions it has been possible to investigate the characteristics of IMF produced by two different types of reaction mechanisms. The data analysis prescriptions for the impact parameter selection allowed to select a well defined set of events; in the study of the Ni+Ni and Ni+Ag reactions it has been possible to select events in which the IMFs are competitively emitted by the decay of the QP and by an intermediate velocity source.

Concerning the disassembly of the QP it has been verified that this system reaches a thermal equilibrium before decaying following a statistical pattern. This point was clarified looking at the experimental angular and energy distributions; isotropic angular distributions and maxwellian shape for the energy distributions give an indication that the thermalization has taken place. A comparison with the SMM predictions strongly support this hypothesis.

The analysed QP systems present the same characteristics in the three considered reactions; in particular their temperature and excitation energy ( $T \simeq 4$  MeV,  $E^* \simeq 4$  MeV/nucleon) suggest the multifragmentation as the main statistical de-excitation channel.

Inside the same nuclear events, in the Ni+Ni, Ni+Ag collisions, IMF production is present also at midvelocity, due to dynamical processes. On the contrary, the Al target seems to be too light to allow the formation of a neck structure, from the overlap of projectile and target during the collision.

The neck IMFs, when compared to the products of the QP decay, show a very different behaviour for what concern the charge distribution and the isotopic content of the fragments. These evidences are taken as a signature of the different nature of the two processes, statistical and dynamical, leading to the formation of IMF.

The charge distribution and the average values of the  $N/Z$  ratio (for different  $Z$  numbers) of the neck IMFs produced in the Ni+Ni and Ni+Ag reactions are very similar.

Once fixed the QP characteristics (size, excitation energy and temperature) and verified that the partner dynamical IMF production present similar features in different reactions, we observe that the production amount of neck IMFs increases with the size of the target nucleus.

Table 1

Temperature parameters extracted from a Maxwellian fit procedure of the isotope energy spectra (typical fit error on extracted values is  $\pm 1$  MeV)

$Z$	$A$	$T_{slope}$ (MeV) (Ni+Al)	$T_{slope}$ (MeV) (Ni+Ni)	$T_{slope}$ (MeV) (Ni+Ag)
3	6	8.4	7.8	8.4
3	7	7.6	9.0	8.2
3	8	7.8	7.8	8.4
4	7	9.5	9.7	10.8
4	9	9.9	10.5	9.8
4	10	10.7	9.7	12.1
5	10	10.9	9.6	10.1
5	11	10.4	10.0	10.9
6	12	7.9	8.7	10.5
6	13	7.4	9.1	10.5

Table 2

Isotopic composition of fragments emitted by the QP's (statistical errors are of the order of a few %)

$Z$	$A$	Ni+Al (%)	Ni+Ni (%)	Ni+Ag (%)
3	6	34.5	41.3	33.7
3	7	39.3	35.3	43.5
3	8	26.2	23.4	22.8
4	7	45.6	54.3	31.0
4	9	36.7	31.0	43.3
4	10	17.7	14.7	25.7
5	10	37.5	40.6	37.1
5	11	52.2	48.1	50.1
5	12	10.3	11.3	12.8
6	11	13.6	17.8	15.6
6	12	44.0	48.3	41.1
6	13	34.8	25.2	31.1
6	14	7.6	8.7	12.2

## References

- [1] "Multifragmentation", Proceedings of the International Workshop 27 on Gross Properties of Nuclei and Nuclear Excitations, Hirschegg, Austria, January 17–23, 1999. GSI, Darmstadt, 1999; W.Reisdorf *et al.*, Phys. Lett. **B595** (2004) 118. M.Veselsky,

Table 3

Average N/Z values of the IMFs emitted from the QP

Z	$\langle N/Z \rangle_{qp(Ni+Al)}$	$\langle N/Z \rangle_{qp(Ni+Ni)}$	$\langle N/Z \rangle_{qp(Ni+Ag)}$
3	1.31	1.27	1.30
4	1.07	1.02	1.16
5	1.15	1.14	1.15
6	1.06	1.04	1.07

Table 4

Temperature and excitation energy of QPs

	T (MeV)	E* (MeV/nucleon)
Ni+Al	3.7±0.2	4.0±0.5
Ni+Ni	3.9±0.2	4.0±0.5
Ni+Ag	4.1±0.2	3.5±0.5

Table 5

Average N/Z values of the neck IMFs

Z	$\langle N/Z \rangle_{Neck(Ni+Ni)}$	$\langle N/Z \rangle_{Neck(Ni+Ag)}$
3	1.50	≥1.44
4	1.43	≥1.36
5	1.26	≥1.26
6	1.25	≥1.18

<http://arXiv.org/abs/nucl-ex/0407002>.

- [2] A.Bonasera, M.Bruno, C.O.Dorso and P.F.Mastinu, *La Rivista del Nuovo Cimento* **23** (2000) 1; P. Chomaz, *Nucl. Phys. A* **685** (2001) 274.
- [3] J. Pochodzalla *et al.*, *Phys. Rev. Lett.* **75** (1995) 1040; P. F. Mastinu *et al.*, *Phys. Rev. Lett.* **76**, (1996) 2646; J. A. Hauger *et al.*, *Phys. Rev. C* **57**, (1998) 764; P.M.Milazzo *et al.*, *Phys. Rev. C* **58** (1998) 953; M. D'Agostino *et al.*, *Nucl. Phys.* **A650**, (1999) 329; M. D'Agostino *et al.*, *Phys. Lett.* **B473** (2000) 219; J.B.Natowitz *et al.*, *Phys. Rev. C* **65**, (2002) 34618; M. D'Agostino *et al.*, *Nucl. Phys.* **A724** (2003) 455.
- [4] A. S. Botvina *et al.*, *Nucl. Phys.* **A475** (1987) 663; J.P. Bondorf *et al.*, *Phys. Rep.* **257** (1995) 133; M. D'Agostino *et al.*, *Phys. Lett.* **B371** (1996) 175; P.M.Milazzo *et al.*, *Phys. Rev. C* **60** (1999) 044606.
- [5] G. Casini *et al.*, *Phys. Rev. Lett.*, **71**, 2567 (1993); C. P. Montoya *et al.*, *Phys. Rev. Lett.*, **73**, 3070 (1994); J. Toke *et al.*, *Phys. Rev. Lett.*, **75**, 2920 (1995); J. F. Dempsey *et al.*, *Phys. Rev. C* **54**, (1996) 1710; Y. Larochelle *et al.*, *Phys. Rev. C* **55**, (1997) 1869; J. Lukasik *et al.*, *Phys. Rev. C* **55**, (1997) 1906; P. Pawlowski *et al.*, *Phys. Rev. C* **57**, (1998) 1711; E. Plagnol *et al.*, *Phys. Rev. C* **61** (1999) 014606; R.Wada *et al.*, *Phys. Rev. C* **62** (2000) 034601; M.Veselsky *et al.*, *Phys. Rev. C* **62** (2000) 041605(R); Y. Larochelle *et al.*, *Phys. Rev. C* **62** (2000) 051602(R); S. Piantelli *et al.*, *Phys. Rev. Lett.*, **88**, (2002) 052701; B. Davin *et al.*, *Phys. Rev. C* **85** (2002) 064614; J.Lukasik *et al.*, *Phys. Lett.* **B566** (2003) 76.
- [6] P.M.Milazzo *et al.*, *Phys. Lett.* **B509** (2001) 204.

- [7] W. Bauer *et al.*, Phys. Rev. Lett., **69**, (1992) 1888; M. Colonna *et al.*, Nucl. Phys., **A583**, (1995) 525; M. Colonna *et al.*, Nucl. Phys., **A589**, (1995) 2671; V. Baran *et al.*, Nucl. Phys., **A703**, (2002) 603.
- [8] E. Migneco *et al.*, Nucl. Instr. and Meth. Phys. Res., **A314** (1992) 31.
- [9] I. Iori *et al.*, Nucl. Instr. and Meth. Phys. Res., **A325** (1993) 458.
- [10] W. Bauer, Phys. Rev. **C51**, (1995) 803.
- [11] Isospin Physics in Heavy Ion Collisions at Intermediate Energies, ed. by Bao-An Li and W. Udo Schroeder, ISBN 1-56072-888-4, Nova Science, New York (2001); H. Mller and B.D. Serot, Phys. Rev. **C52**, (1995) 2072; B.-A. Li, C.M. Ko, and W. Bauer, Int. J. Mod. Phys. **E7**, (1998) 147; W.P. Tan *et al.*, Phys. Rev. **C64**, (2001) 051901(R).
- [12] P.M.Milazzo *et al.* Nucl. Phys. **A703**, (2002) 466.
- [13] X.Campi *et al.*, Phys. Rev. **C50**, (1994) R2680.
- [14] E.Vient *et al.* Nucl. Phys. **A700**, (2002) 555.
- [15] A.Mangiarotti *et al.*, Phys. Rev. Lett., **93**, (2004) 232701;
- [16] S.Albergo *et al.*, Nuovo Cimento **89** (1985) 1.
- [17] M.B.Tsang *et al.*, Phys. Rev. Lett., **78** (1997) 3836;
- [18] M.B.Tsang *et al.*, NSCL-MSU Report n.1035 (1997).
- [19] P.M.Milazzo *et al.*, Phys. Rev. **C60**, (1999) 044606.
- [20] M. Belkacem *et al.*, Phys. Rev. **C52**, (1995) 271.